Available online at www.sciencedirect.com

ScienceDirect

Ceramics International 38S (2012) S363–S368

CERAMICS INTERNATIONAL

www.elsevier.com/locate/ceramint

Structure, ferroelectric properties, and electric field-induced large strain in lead-free $Bi_{0.5}(Na,K)_{0.5}TiO_3$–$(Bi_{0.5}La_{0.5})AlO_3$ piezoelectric ceramics

Aman Ullah [a], Chang Won Ahn [b], Sun Young Lee [a], Jin Soo Kim [a], Ill Won Kim [a,*]

[a] Department of Physics, University of Ulsan, Ulsan 680-749, South Korea
[b] Convergence Components R&D Division, KETI, Seongnam 463-816, South Korea

---

Abstract

Lead-free $(1-x)Bi_{0.5}(Na_{0.78}K_{0.22})_{0.5}TiO_3$–$x(Bi_{0.5}La_{0.5})AlO_3$ (BNKT–BLA) piezoelectric ceramics with x ranging from 0 to 0.030 were synthesized by a conventional solid state reaction method. The effect of $(Bi_{0.5}La_{0.5})AlO_3$ addition on the structure, ferroelectric properties, and electric field-induced strain were investigated. In the studied composition range, the XRD patterns revealed a single perovskite phase with tetragonal symmetry. However, the tetragonality (c/a) of the BNKT ceramics significantly decreased as the BLA content was increased. The polarization and strain hysteresis loops indicate that the ferroelectric order of the BNKT ceramics was significantly disrupted by the addition of BLA, leading to degradation in the remnant polarization and coercive field. However, the destabilization of the ferroelectric order is accompanied by significant enhancements in the bipolar and unipolar strains. A large electric field-induced strain ($S = 0.40\%$) and a corresponding normalized strain ($d_{33}^* = S_{max}/E_{\max} = 579\,\text{pm/V}$) were observed under 70 kV/cm at a composition of $x = 0.010$.

Keywords: A. Powder solid state reaction; A. Sintering; C. Ferroelectric properties; C. Piezoelectric properties

---

1. Introduction

Lead oxide-based ferroelectric ceramics, such as $Pb(Zr,Ti)O_3$ (PZT), are widely used as piezoelectric actuators, sensors, and transducers due to their high-performance piezoelectric properties [1,2]. However, with respect to legislation, lead is considered to be toxic and its use is banned for many commercial applications. As such, lead-free piezoelectrics have become the focus of intense interest in both industry and academia [3,4].

The ceramic $Bi_{0.5}Na_{0.5}TiO_3$ (BNT) with a rhombohedral perovskite structure is considered to be a good lead-free piezoelectric ceramic candidate due to its strong ferroelectric behavior at room temperature [5]. However, poling of pure BNT is difficult due to its high conductivity. Furthermore, the piezoelectric properties of BNT are too low for practical applications. To improve its piezoelectric properties, BNT has been modified with other perovskite materials such as $BaTiO_3$ (BT) [6,7], $SrTiO_3$ (ST) [8,9], $(Bi_{0.5}K_{0.5})TiO_3$ (BKT) [10–13], $NaNbO_3$ [14], $KNbO_3$ [15], and $Bi_{0.5}Na_{0.5}TiO_3$–$BaTiO_3$–$K_{0.5}Na_{0.5}NbO_3$ (BNT–BT–KNN) [16]. Among these modified BNT-based ceramics, the BNT–BKT class of materials has received a great deal of attention due to their excellent ferroelectric and piezoelectric properties near the rhombohedral–tetragonal morphotropic phase boundary (MPB) with $0.16 \le x \le 0.20$ [11–13]. In the BNT–BKT binary system, a relatively high strain of ~0.23% and a corresponding d_{33}^* of ~291 pm/V have been observed for a material at the tetragonal side $Bi_{0.5}(Na_{0.78}K_{0.22})_{0.5}TiO_3$ of the MPB. Such a material is aptly suited for use in electromechanical devices [17,18]. Thus, ceramics with a composition at the tetragonal side $Bi_{0.5}(Na_{0.78}K_{0.22})_{0.5}TiO_3$ (BNKT) of the MPB were selected as the matrix material in this study.

Recent theoretical calculations predict that $BiAlO_3$ (BA) has a very large spontaneous polarization of about 76 $\mu C/cm^2$ and a Curie temperature of approximately 800 K [19]. Furthermore, theoretical calculations predict that the BA crystal structure will have perovskite-like rhombohedral symmetry [19]. Zylberberg et al. have synthesized BA and have confirmed that it is indeed ferroelectric and has a Curie temperature $T_c > 520\,^{\circ}C$ [20]. However, the poor thermal stability and extreme conditions used to synthesize BA limit its usability in technological

---

* Corresponding author. Tel.: +82 52 259 2323; fax: +82 52 259 1693.
E-mail address: kimiw@mail.ulsan.ac.kr (I.W. Kim).

0272-8842/$36.00 © 2011 Elsevier Ltd and Techna Group S.r.l. All rights reserved.
doi:10.1016/j.ceramint.2011.05.013

applications [20]. Therefore, a favorable approach is to stabilize BA by incorporating it into other perovskite materials in order to form solid solutions. Watanaba et al. [21] have fabricated $(1-x)Bi_{0.5}Na_{0.5}TiO_3–xBiAlO_3$ ferroelectric ceramics and evaluated their electrical properties. Recently, Yu and Ye have synthesized a $(1-x)(Na_{0.5}Bi_{0.5})TiO_3–xBiAlO_3$ (NBT–BA) ceramic system and observed excellent ferroelectric and piezoelectric properties in comparison to pure NBT ceramics [22]. Hiruma et al. [23] recently synthesized $(1-x)(Bi_{1/2}Na_{1/2})TiO_3–xBa(Al_{1/2}Nb_{1/2})O_3$ (BNT–BAN) solid solution ceramics and reported a maximum strain of approximately 0.40% and a corresponding normalized strain d^*_{33} of 533 pm/V at $x = 0.055$.

In this study, a new lead-free solid solution $(1-x)Bi_{0.5}(Na_{0.78}K_{0.22})_{0.5}TiO_3–x(Bi_{0.5}La_{0.5})AlO_3$ (BNKT–BLA) was developed by partially substituting La^{3+} for Bi^{3+} in the A-site of $BiAlO_3$ ceramics. The BNKT–BLA ceramics were fabricated by a conventional solid state reaction method. The effect of $(Bi_{0.5}La_{0.5})AlO_3$ (BLA) content on the crystalline structure, microstructure, ferroelectric properties, and electric field-induced strain were investigated. The goal of this study is to search for new lead-free materials with a high electric field-induced strain response.

2. Experimental

The $(1-x)Bi_{0.5}(Na_{0.78}K_{0.22})_{0.5}TiO_3–x(Bi_{0.5}La_{0.5})AlO_3$ ($x = 0–0.030$) piezoelectric ceramics were synthesized by a conventional solid state reaction method using Bi_2O_3, TiO_2, Al_2O_3, La_2O_3 (99.9%, High Purity Chemicals), Na_2CO_3 (99.9%, Cerac Specialty Inorganics), and K_2CO_3 (≥99%, Sigma–Aldrich) as the starting raw materials. Before weighing was performed, the powders were dried in an oven at 100 °C for 12 h. The BNKT and BLA were first prepared separately, and then calcined at 850 °C for 2 h. Both materials were weighed according to the stoichiometric formula and ball milled for 24 h in ethanol with zirconia balls. The dried slurries were calcined at 800 °C for 2 h and then ball milled again for 24 h. The powders were pulverized, mixed with an aqueous polyvinyl alcohol (PVA) solution, and pressed into green disks with diameters of 13 mm under a pressure of 150 MPa.

Sintering was carried out at 1150–1170 °C for 2 h in covered alumina crucibles. To prevent the vaporization of Bi, Na, and K, the disks were embedded in a powder of the same composition. The crystal structures of the ceramics were characterized by X-ray diffractometry (XRD, X'pert PRO MRD, Philips). Scanning electron microscopy (JSM-5610LV) was employed so as to examine the surface morphology of polished and thermally etched samples. The sintered disks were polished in order to measure their electrical properties. Silver paste was applied on both surfaces of the disks as an electrode. After applying the silver, the disks were fired at 700 °C for 30 min. Ferroelectric hysteresis loops were measured in silicon oil using a conventional Sawyer–Tower circuit in order to apply an electric field with a triangular waveform. The electric field-induced strain was measured with a linear variable differential transducer (LVDT, Mitutoyo MCH-331 & M401). A high voltage amplifier (Trek, 610E) driven by a waveform generator (Agilent 33250A) was employed to supply the voltage. Using the unipolar strain–field curves, the normalized strain ($d^*_{33} = S_{max}/E_{max}$) was calculated from the ratio of the maximum strain to the maximum electric field.

3. Results and discussion

The X-ray diffraction patterns of the $(1-x)$BNKT–xBLA ceramics ($x = 0.00–0.030$) as 2θ was varied over a range of 20–80° are shown in Fig. 1(a). All the ceramics possess a single phase perovskite structure and no second phases can be detected. The absence of second phases indicates that the La^{3+} and Al^{3+} ions diffused into the BNKT lattice to form a homogeneous solid solution. Detailed XRD scans for the BNKT–BLA ceramics in the 2θ range of 35–50° are shown in Fig. 1(b). In agreement with previously reported studies [11,13,17,18], the BNKT samples had tetragonal symmetry, as evidenced by the splitting of (0 0 2)/(2 0 0) peaks at a 2θ angle of around 46° and the existence of a single (1 1 1) peak at a 2θ angle of approximately 40°. With an increase in the BLA content, the tetragonal distortion gradually decreased and the (0 0 2) peak steadily became weak. However, the (0 0 2) peak did not completely merge with the (2 0 0) peak, even at higher concentrations (i.e. $x = 0.030$). This behavior became clearer after an analysis of the calculated lattice parameters and tetragonality (c/a), as shown in Fig. 2.

The effect of BLA content on the lattice parameters, a and c, calculated at the (0 0 2)/(2 0 0) peaks and the tetragonality (c/a) of the BNKT–BLA ceramics is shown in Fig. 2. It is evident from Fig. 2 that the lattice constant 'c' and the tetragonality (c/a) significantly decreased with an increase in the BLA content. However, the lattice constant 'a' only changed slightly. The decreasing trend in tetragonality clearly indicates that the addition of BLA decreased the lattice anisotropy of the BNKT ceramic.

SEM micrographs of the polished and thermally etched surfaces of the $(1-x)$BNKT–xBLA ceramics with $x = 0$, 0.003, 0.005, 0.010, 0.025, and 0.030 are shown in Fig. 3.

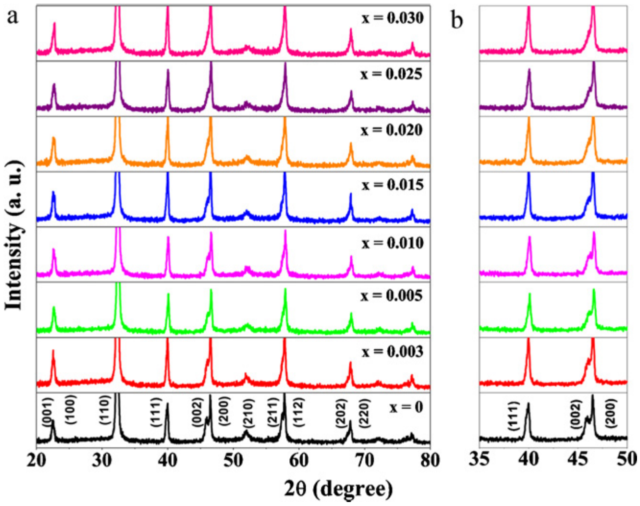

Fig. 1. X-ray diffraction patterns of the $(1-x)$BNKT–xBLA ceramics ($x = 0–0.030$) in the 2θ range of (a) 20–80° and (b) 35–50°.

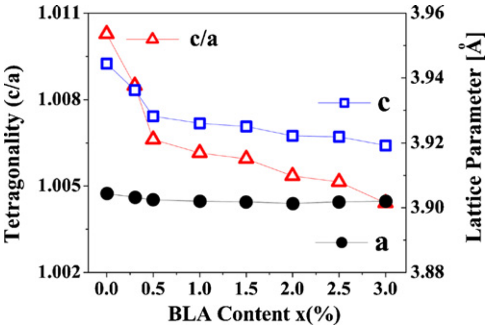

Fig. 2. Lattice constants, *a* and *c*, and the tetragonality (*c*/*a*) as functions of *x* in the (1 − *x*)BNKT–*x*BLA ceramics.

From the SEM images, it is evident that all the samples are considerably dense with a well-developed microstructure and a granular morphology. The addition of BLA has no significant influence on the grain size and grain morphology. However, the average grain size slightly increases and somewhat coarse grains are formed at higher BLA contents. The effect of BLA on grain growth in the present ceramics is similar to that observed for $(Bi_{0.94-x}La_xNa_{0.94})_{0.5}Ba_{0.06}TiO_3$ ceramics, where the grain size slightly increased after the substitution of La^{3+} for Bi^{3+} [24].

The *P*–*E* hysteresis loops of the (1 − *x*)BNKT–*x*BLA ceramics with $x = 0$, 0.003, 0.005, 0.010, 0.015, and 0.030 measured at room temperature are shown in Fig. 4(a). BNKT–BLA ceramics without the addition of BLA display typical well-saturated *P*–*E* hysteresis loops with maximum and remnant polarizations of 41 $\mu C/cm^2$ and 29 $\mu C/cm^2$, respectively, and a coercive field of 26 kV/cm. As evident in the hysteresis curves, BLA exerts a significant influence on the shape and polarization values of the *P*–*E* loop. The composition-dependent remnant polarization (P_r), maximum polarization (P_m), and coercive field (E_c) of the BNKT–BLA ceramics are shown in Fig. 4(b). The profiles of the *P*–*E* hysteresis loops are in good agreement with the XRD results. It should be noted that, at 0.3 mol (%) BLA, the tetragonality sharply decreased (see Fig. 2). Such a sharp decrease resulted in a drastic reduction in the remnant polarization, from 29 for BNKT to 9 $\mu C/cm^2$. The coercive field also decreased, from 26 to 11 kV/cm, and the hysteresis curve became slightly pinched and slimmer. The maximum polarization decreased from 41 to 36 $\mu C/cm^2$. At a higher BLA content ($x = 0.030$), the *P*–*E*

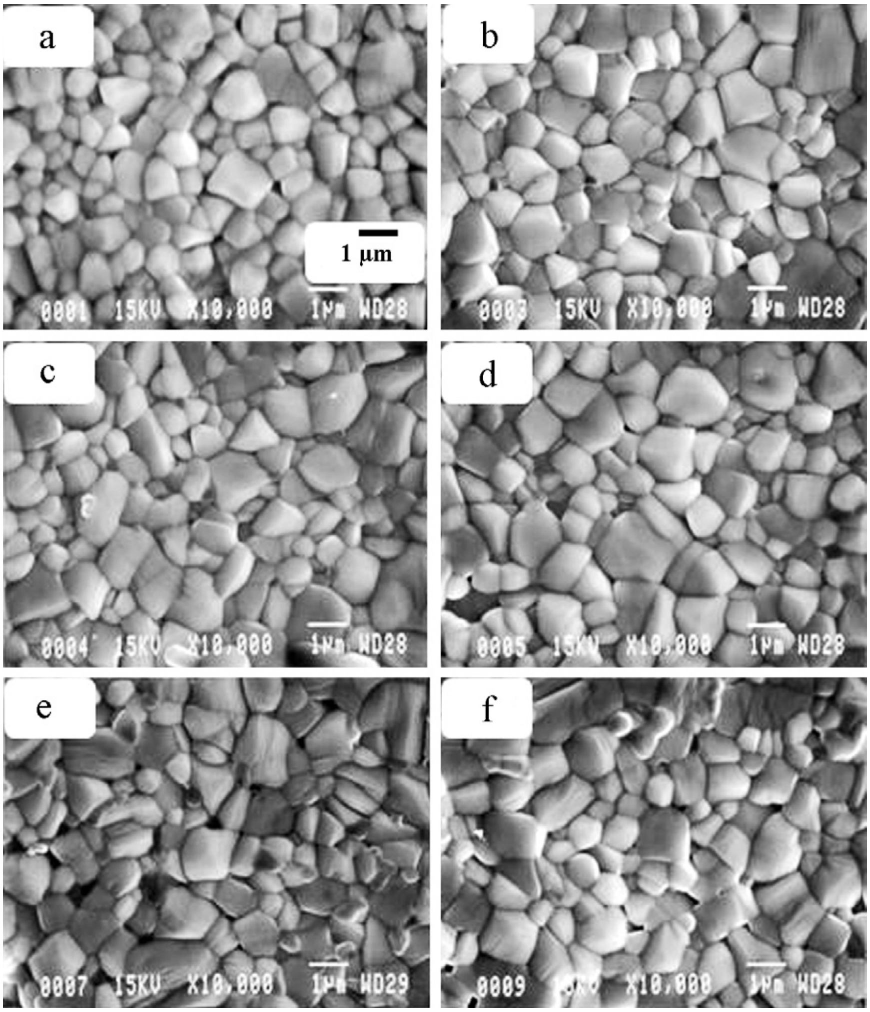

Fig. 3. SEM micrographs of the (1 − *x*)BNKT–*x*BLA ceramics with (a) $x = 0$, (b) $x = 0.003$, (c) $x = 0.005$, (d) $x = 0.010$, (e) $x = 0.025$, and (f) $x = 0.030$.

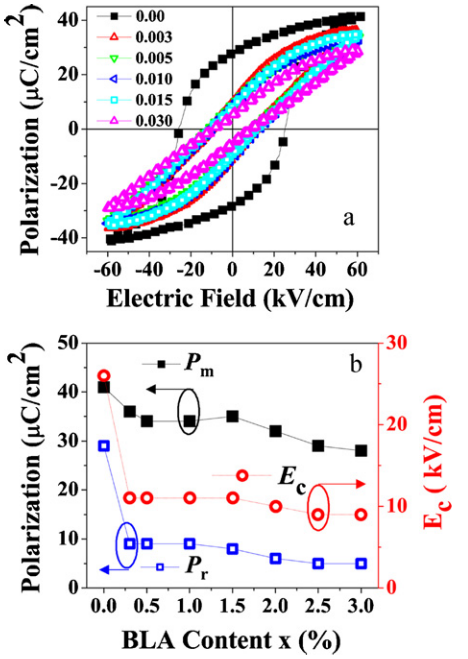

Fig. 4. (a) Room temperature *P–E* hysteresis loops of the $(1-x)$BNKT–xBLA ceramics with $x=0$, 0.003, 0.005, 0.010, 0.015, and 0.030. (b) Maximum polarization (P_m), remnant polarization (P_r), and coercive field (E_c) as functions of x in the $(1-x)$BNKT–xBLA ceramics.

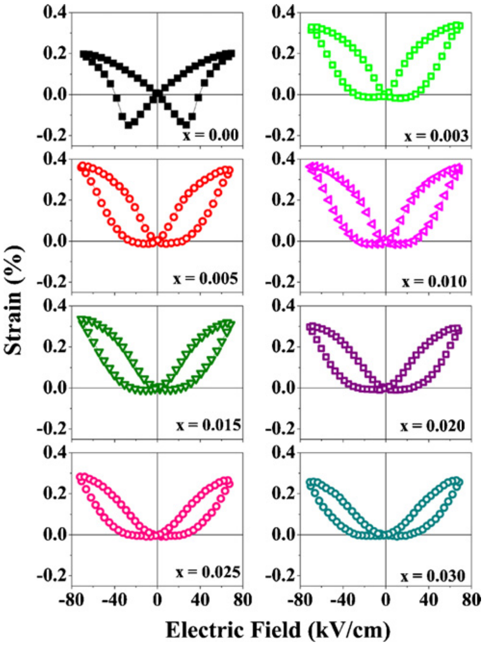

Fig. 5. The bipolar *S–E* loops of the $(1-x)$BNKT–xBLA ceramics.

hysteresis loop became slimmer and P_r and E_c values of 5 μC/cm^2 and 9 kV/cm, respectively, were observed. The maximum polarization also decreased to 28 μC/cm^2. Such significant decreases in the polarization values are an indicator that the ferroelectric order, which was dominant in BNKT, is disrupted by the addition of BLA. However, the presence of traces of ferroelectric order at a higher BLA content at zero electric field is evident because the remnant polarization ($P_r = 5$ μC/cm^2 at $x = 0.030$) is not negligible. The slightly pinched *P–E* hysteresis loops and the destabilization of the ferroelectric order in BNKT–BLA ceramics may be attributed to the possible existence of non-polar regions induced by the BLA content. This phenomenon is similar to that observed in other BNT-based ceramics [25–27]. Recently, Zheng et al. reported that a high substitution of La^{+3} for Bi^{+3} led to the existence of non-polar regions in $(Bi_{0.94-x}La_xNa_{0.94})_{0.5}Ba_{0.06}TiO_3$ ceramics [24]. Although the ferroelectric order in the BNKT–BAL system is disrupted by chemical modification, samples in the composition range of $0.003 \le x \le 0.015$ exhibits saturated *P–E* hysteresis loops. Such a result may be an indicator that different polarization states (ferroelectric and non-polar) coexist in this composition range and the free energy of the ferroelectric phase may be comparable to that of the non-polar phase at zero electric field. Thus, the ferroelectric phase can be easily induced by an external electric field and saturated at 60 kV/cm. At a higher BLA concentration ($x = 0.030$), the maximum polarization significantly decreased from 41 to 28 μC/cm^2. This implies that the ferroelectric–non-polar phase transformation may not be complete at the applied electric field. As such, a slimmer *P–E* hysteresis loop was observed at higher BLA concentrations.

The bipolar strain hysteresis loops of the BNKT–BLA ceramics at 70 kV/cm are shown in Fig. 5. It is evident that BNKT without any addition of BLA exhibits a butterfly-shaped strain hysteresis loop that is typical for ferroelectric materials. A maximum strain of 0.20% and a negative strain (the difference between the zero field strain and the lowest strain which is only visible in the bipolar cycle) [28] of −0.14% were observed in the BNKT samples with no BLA addition. In contrast, as the BLA content is increased, the strain loops show a drastic deviation from typical ferroelectric behavior. This is evident from the absence of negative strain that is closely related to domain back switching during bipolar cycles. Instead, a pronounced enhancement in the maximum strain response was observed. Maximum strains of 0.35%, 0.37%, 0.38%, and 0.34% were observed for $x = 0.003$, 0.005, 0.010, and 0.015, respectively. Beyond this narrow region, the maximum strain gradually decreased while the negative strain nearly vanished. Zhang et al. [28] recently reported that the $0.94(Bi_{0.5}Na_{0.5})$-TiO_3–$0.06BaTiO_3$ (BNT–BT) system delivers a large strain response when a small amount of BNT is replaced by $(K_{0.5}Na_{0.5})NbO_3$ (KNN). However, the emergence of such a large strain is accompanied by a significant reduction in the remnant polarization and negative strain. Jo et al. [25] proposed that the large strain response in the KNN-modified BNT–BT system may be due to the combined effects of the intrinsically high poling strain and the presence of a non-polar phase that easily transforms to a ferroelectric phase under an electric field due to its comparable free energy. In a recent report from Seifert et al. [26], a large strain was observed in $(Bi_{1/2}Na_{1/2})TiO_3$–$(Bi_{1/2}K_{1/2})TiO_3$–$(K_{0.5}Na_{0.5})NbO_3$ ceramics. The researchers found that the ferroelectric order of BNT–BKT is significantly disrupted by the addition of KNN as a replacement for BNT. The destabilization of the ferroelectric order was accompanied by an enhancement in the unipolar strain. In the present study,

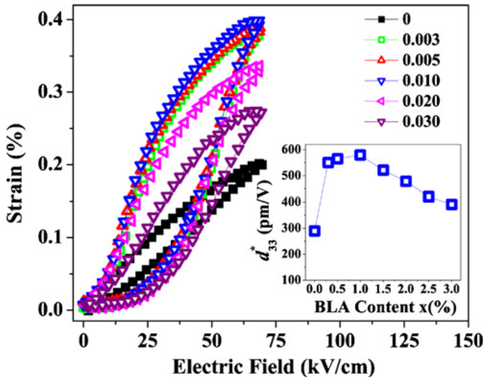

Fig. 6. The unipolar *S*–*E* loops of the (1 − *x*)BNKT–*x*BLA ceramics with $x = 0$, 0.003, 0.005, 0.010, 0.020, and 0.030. The composition dependent normalized strain d^*_{33} of the BNKT–BLA ceramics is shown in the inset.

the abrupt increase in the strain response at $x = 0.003$–0.015 is possibly due to the degree of inducible ferroelectric order under the electric field once the ferroelectric order at zero field becomes unstable by the replacement of BNT with a small amount of BLA. This phenomenon is similar to that observed in the BNT–BT–KNN [25,28], $Bi_{0.5}(Na_{0.78}K_{0.22})_{0.5}(Ti_{1-x}Zr_x)O_3$ [27], and BNT–BKT–KNN ceramic systems [26].

The unipolar electric field-induced strain curves of the $(1-x)$BNKT–xBA ceramics with $x = 0$, 0.003, 0.005, 0.010, 0.020, and 0.030 at 70 kV/cm are shown in Fig. 6. The normalized strain ($d^*_{33} = S_{max}/E_{max}$) of the BNKT–BLA ceramics for all studied compositions is summarized in the inset of Fig. 6 and was calculated from the ratio of the maximum strain (S_{max}) to the maximum electric field (E_{max}) [28].

As previously discussed, BLA addition disrupts the ferroelectric order of BNKT ceramics, resulting in a slightly pinched hysteresis loop and a significant decrease in the remnant polarization, coercive field, and negative strain. Such a scenario favors stabilization of the non-polar phase. However, the destabilization of the ferroelectric order is accompanied by a significant enhancement in the electric field-induced strain response. A large strain ($S = 0.40\%$) and corresponding normalized strain ($d^*_{33} = 579\,\text{pm/V}$) were observed at a composition of $x = 0.010$. The values of d^*_{33} for the compositions $x = 0.003$, 0.005, 0.010, and 0.015 are 550, 565, 579, and 521, respectively. These values are higher (>500 pm/V) in the studied composition range, implying that a strain derived under an electric field arises from a common origin in this composition range ($0.003 \le x \le 0.015$). It is suggested that samples with these compositions have mixed ferroelectric and non-polar phases, as evidenced by their slightly pinched hysteresis loops and almost similar polarization values (i.e. remnant polarization, coercive field, and maximum polarization). The coexistence of different polarization states in this system may indicate that the free energy of both phases is comparable. The field-induced strain caused by the ferroelectric–non-polar phase transition is nearly twice ($S = 0.40\%$, at $x = 0.010$) that caused by ferroelectric domain switching alone ($S = 0.20\%$, at $x = 0$). Therefore, on the basis of the *P*–*E* hysteresis loops and the *S*–*E* loops, the results of this study suggest that this large electric field-induced strain is due to the coexistence of ferroelectric and non-polar phases.

4. Conclusion

Lead-free $(1-x)Bi_{0.5}(Na_{0.78}K_{0.22})_{0.5}TiO_3$–$x(Bi_{0.5}La_{0.5})AlO_3$ piezoelectric ceramics were successfully synthesized by a solid state reaction method. The results of X-ray diffractometry revealed that the La^{3+} and Al^{3+} diffused into the $Bi_{0.5}(Na_{0.78}K_{0.22})_{0.5}TiO_3$ lattice to form a homogeneous solid solution with a single-phase tetragonal perovskite structure. An increase in the BLA content significantly reduced the tetragonality of the BNKT lattice. The ferroelectric order in the BNKT ceramics was significantly disrupted by the addition of BLA, resulting in a drastic degradation in the remnant polarization, coercive field, and negative strain. However, the degradation of the polarization values was accompanied by a significant enhancement in the strain behavior. In particular, a very large electric field-induced strain ($S = 0.40\%$) and a corresponding normalized strain ($d^*_{33} = 579\,\text{pm/V}$) were obtained at $x = 0.010$.

Acknowledgements

This research was financially supported by the Ministry of Education, Science and Technology (MEST) and the Korea Institute for Advancement of Technology (KIAT) through the Human Resource Training Project for Regional Innovation. The authors also acknowledge the Priority Research Centers Program through the National Research Foundation of Korea (NRF) funded by the Ministry of Education, Science and Technology (2009-0093818).

References

[1] G.H. Haertling, Ferroelectric ceramics: history and technology, Journal of the American Ceramics Society 82 (1999) 797–818.
[2] S.E. Park, T.R. Shrout, Ultrahigh strain and piezoelectric behavior in relaxor based ferroelectric single crystals, Journal of Applied Physics 82 (1997) 1804–1811.
[3] Y. Li, K.S. Moon, C.P. Wong, Electronics without lead, Science 308 (2005) 1419–1420.
[4] L.E. Cross, Lead-free at last, Nature 432 (2004) 24–25.
[5] G.A. Smolenskii, V.A. Isupov, A.I. Agranovskaya, N.N. Krainik, New ferroelectrics of complex composition, Soviet Physics Solid State 2 (1961) 2651–2654.
[6] T. Takenaka, K. Maruyama, K. Sakata, $(Bi_{1/2}Na_{1/2})TiO_3$–$BaTiO_3$ system for lead-free piezoelectric ceramics, Japanese Journal of Applied Physics 30 (1991) 2236–2239.
[7] Y.M. Chiang, G.W. Farrey, A.N. Soukhojak, Lead-free high-strain single-crystal piezoelectrics in the alkaline–bismuth–titanate perovskite family, Applied Physics Letters 73 (1998) 3683–3685.
[8] K. Sakata, Y. Masuda, Ferroelectric and antiferroelectric properties of $(Na_{0.5}Bi_{0.5})TiO_3$–$SrTiO_3$ solid solution ceramics, Ferroelectrics 7 (1974) 347–349.
[9] Y. Hiruma, Y. Imai, Y. Watanabe, H. Nagata, T. Takenaka, Large electrostrain near the phase transition temperature of $(Bi_{0.5}Na_{0.5})TiO_3$–$SrTiO_3$ ferroelectric ceramics, Applied Physics Letters 92 (2008) 262904.
[10] O. Elkechai, M. Manier, J.P. Mercurio, $Na_{0.5}Bi_{0.5}TiO_3$–$K_{0.5}Bi_{0.5}TiO_3$ (NBT–KBT) system: a structural and electrical studies, Physica Status Solidi A 157 (1996) 499–506.

[11] A. Sasaki, T. Chiba, Y. Mamiya, E. Otsuki, Dielectric and piezoelectric properties of $(Bi_{0.5}Na_{0.5})TiO_3–(Bi_{0.5}K_{0.5})TiO_3$ system, Japanese Journal of Applied Physics 38 (1999) 5564–5567.

[12] Z. Yang, B. Liu, L. Wei, Y. Hou, Structure and electrical properties of $(1 - x)Bi_{0.5}Na_{0.5}TiO_3–xBi_{0.5}K_{0.5}TiO_3$ ceramics near morphotropic phase boundary, Materials Research Bulletin 43 (2008) 81–89.

[13] W. Zhao, H. Zhou, Y. Yan, D. Liu, Morphotropic phase boundary study of the BNT–BKT lead-free piezoelectric ceramics, Key Engineering Materials 368–372 (2008) 1908–1910.

[14] T. Takenaka, T. Okuda, K. Takegahara, Lead-free piezoelectric ceramics based on $(Bi_{1/2}Na_{1/2})TiO_3–NaNbO_3$, Ferroelectrics 196 (1997) 175–178.

[15] H. Ishii, H. Nagata, T. Takenaka, Morphotropic phase boundary and electrical properties of bismuth sodium titanate–potassium niobate solid-solution ceramics, Japanese Journal of Applied Physics 40 (2001) 5660–5663.

[16] S.T. Zhang, A.B. Kounga, E. Aulbach, Giant strain in lead-free piezoceramics $Bi_{0.5}Na_{0.5}TiO_3–BaTiO_3–K_{0.5}Na_{0.5}NbO_3$ system, Applied Physics Letters 91 (2007) 112906.

[17] K. Yoshii, Y. Hiruma, H. Nagatha, T. Takenaka, Electrical properties and depolarization temperature of $(Bi_{1/2}Na_{1/2})TiO_3–(Bi_{1/2}K_{1/2})TiO_3$ lead-free piezoelectric ceramics, Japanese Journal of Applied Physics 45 (2006) 4493–4496.

[18] Y. Hiruma, H. Nagatha, T. Takenaka, Phase diagrams and electrical properties of $(Bi_{1/2}Na_{1/2})TiO_3$-based solid solution, Journal of Applied Physics 104 (2008) 124106.

[19] P. Baettig, C.F. Schelle, R. LeSar, U.V. Waghmare, N.A. Spaldin, Theoretical prediction of new high-performance lead-free piezoelectrics, Chemistry of Materials 17 (2005) 1376–1380.

[20] J. Zylberberg, A.A. Belik, E. Takayama-Muromachi, Z.-G. Ye, Bismuth aluminate: a new high-T_c lead-free piezo-/ferroelectric, Chemistry of Materials 19 (2007) 6385–6390.

[21] Y. Watanaba, Y. Hiruma, H. Nagata, T. Takenaka, Fabrication and electrical properties of $(Bi_{1/2}Na_{1/2})TiO_3–BiAlO_3$ ferroelectric ceramics, Key Engineering Materials 388 (2009) 229–232.

[22] H. Yu, Z.-G. Ye, Dielectric ferroelectric and piezoelectric properties of the lead-Free $(1 - x)(Na_{0.5}Bi_{0.5})TiO_3–xBiAlO_3$ solid solution, Applied Physics Letters 93 (2008) 112902.

[23] Y. Hiruma, H. Nagata, T. Takenaka, Formation of morphotropic phase boundary and electrical properties of $(Bi_{1/2}Na_{1/2})TiO_3–Ba(Al_{1/2}Nb_{1/2})O_3$ solid solution ceramics, Japanese Journal of Applied Physics 48 (2009) 09KC08.

[24] Q. Zheng, C. Xu, D. Lin, D. Gao, K.W. Kwok, Piezoelectric and ferroelectric properties of $(Bi_{0.94-x}La_xNa_{0.94})_{0.5}Ba_{0.06}TiO_3$ lead-free ceramics, Journal of Physics D: Applied Physics 41 (2008) 125411.

[25] W. Jo, T. Granzow, E. Aulbach, J. Rodel, D. Damjanovic, Origin of the large strain response in $(K_{0.5}Na_{0.5})NbO_3$-modified $(Bi_{0.5}Na_{0.5})TiO_3–BaTiO_3$ lead-free piezoceramics, Journal of Applied Physics 105 (2009) 094102.

[26] K.T.P. Seifert, W. Jo, J. Rodel, Temperature-insensitive large strain of $(Bi_{1/2}Na_{1/2})TiO_3–(Bi_{1/2}K_{1/2})TiO_3–(K_{0.5}Na_{0.5})NbO_3$ lead-free piezoceramics, Journal of the American Ceramics Society 93 (2010) 1392–1396.

[27] A. Hussain, C.W. Ahn, J.S. Lee, A. Ullah, I.W. Kim, Large electric-field-induced strain in Zr-modified lead-free $Bi_{0.5}(Na_{0.78}K_{0.22})_{0.5}TiO_3$ piezoelectric ceramics, Sensors and Actuators A: Physical 158 (2010) 84–89.

[28] S.-T. Zhang, A.B. Kounga, E. Aulbach, T. Granzow, W. Jo, H.-J. Kleebe, J. Rodel, Lead-free piezoceramics with giant strain in the system $Bi_{0.5}Na_{0.5}TiO_3–BaTiO_3–K_{0.5}Na_{0.5}NbO_3$. I. Structure and room temperature properties, Journal of Applied Physics 103 (2008) 034107.